Journal of Ceramic Processing Research. Vol. 8, No. 1, pp. 64~69 (2007)

JOURNAL OF
Ceramic
Processing Research

The frequency effect on atmospheric pressure RF discharge surface modification

A.F. Alexandrov, E.A. Kralkina, V.B. Pavlov, V.P. Savinov, V. Yu. Sergeenko, I.B. Timofeev, G.E. Bugrov[a], K.V. Vavilin[a], V. Yu. Plaksin[b], Young Son Mok[b] and Heon-Ju Lee[b,*]
Physical Faculty of Moscow State University, Russia
[a]Moscow State Institute of Radioengineering, Electronics and Automation (Technical University), Russia
[b]College of Engineering, Cheju National University, Korea

The physical mechanism of RF discharge at atmospheric pressure was studied at discharge frequencies of 13.56 MHz and 0.6 MHz. The discharge at 0.6 MHz had a clear filamentary structure, while discharge at 13.6 MHz had no separate filaments. The influence of discharge on the properties of polymer surfaces was also investigated, using two surface property indicators, the contact angle with water and adhesion strength. As a result of sample processing in the discharge, the wetting angle of polytetrafluorethylene (PTFE), polyethylene (PE), polyimide (PI) and polyvinyl chloride (PVC) decreased to 40°, 20°, 20° and 25°, respectively, and the adhesion of PTFE increased four fold.

Key words: RF discharge, voltage-current characteristics, adhesion, contact angle.

Introduction

In recent years, the tendency has become evident to develop and utilize discharges at atmospheric pressure in industry especially for plasma chemical applications and the surface modification of materials. A review of the literature [1, 2] devoted to this subject, on the one hand illustrates great potential of such discharges and on the other hand demonstrates a lack of detailed understanding of the physical processes in atmospheric pressure discharges and of the mechanisms of its influence on material surfaces. This paper presents results obtained in a systematic study of atmospheric RF discharge parameters together with results of the influences of discharges on material surface characteristics. The basic goal of these investigations is the development of an extended pulsating discharge operating at atmospheric pressure over a wide range of working frequencies, with high stability and uniformity along a discharge electrode.

Discharge Configuration and Experimental Procedure

Discharges at frequencies of 13.56 MHz and 0.6 MHz at atmospheric pressure were examined. Two types of discharge configuration were used in the experiments. The first configuration corresponds to the pin-plate geometry, shown in Fig. 1. The discharge was ignited between the pin (1) and the grounded metal plate (2), separated by an air gap ranging 4-15 mm. In some experiments, a dielectric layer (3) covered the metal plate. Additional gas flow was supplied through a gas distributor (4). Ignition and sustaining of the discharge RF power supplies (5) with working frequencies of 0.6 MHz and 13.6 MHz were connected to the electrodes of 1 and 2 through the matching box (6).

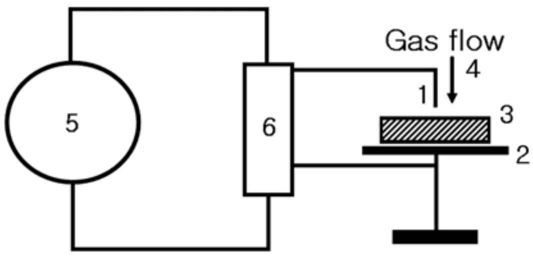

Fig. 1. Diagram of pin-plate discharge experiment: 1-pin, 2-plate, 3-sample, 4-gas distributor, 5-RF generator, 6-matching box.

The second type of discharge was a modification of a previously developed unit, designed to produce a large area uniform plasma for technological applications, mainly surface treatment. This device was used to generate prolonged discharges in this study and is shown in Fig. 2. The ignition electrode (1) initiated a discharge between the metal string (3) and the metal plate (2). The thickness of electrodes was about 0.5 mm. The airflow having longitudinal and transversal components of velocity (in respect to the primary discharge) provided the necessary homogeneity of the discharge.

The velocity of the pin-plate discharge airflow was 0-100 m/s. At prolonged discharge, air velocities of 10-100 m/s were used. Increasing air velocity above 100

*Corresponding author:
Tel : +82-64-754-3642
Fax: +82-64-757-9276
E-mail: hjlee@cheju.ac.kr

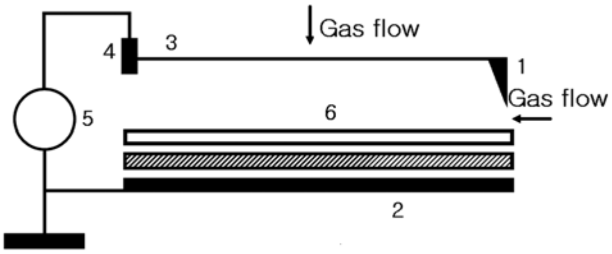

Fig. 2. Diagram of string-plate discharge experiment: 1-ignition electrode, 2-plate, 3,4-working and feeding electrodes, 5-RF generator, 6-sample.

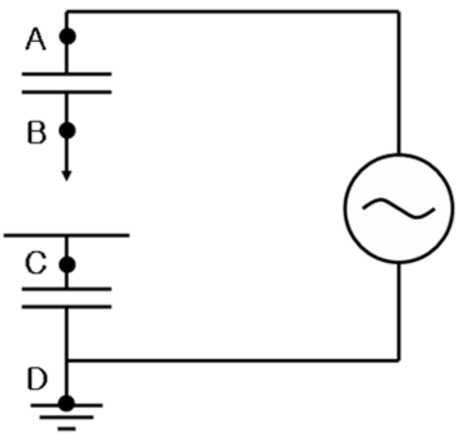

Fig. 3. Diagram of electrical measurements.

m/s lead to rapid removal of charged particles from the ungrounded electrode, and as a result, significantly shrank the discharge area.

To study the discharge properties, the time dependencies of applied voltage and discharge current, volt-ampere characteristics and time averaged potential differences between the plasma and electrodes were measured using the electrical scheme shown in Fig. 3. The RF current and RF voltage supplied to the discharge electrodes were measured using a current probe and RF voltage divider and the signals were registered on a computer equipped with RF analog to digital converter (ADC). RF voltage (V) and DC voltage (U) between points A, B, C were measured utilizing RF voltage dividers and cathode voltmeters. The time averaged potential difference between the plasma and electrode B, U_{BPl} was calculated using formula 1:

$$U_{BPl}=\frac{\left[\frac{V_{BC}}{V_{AB}C_{AB}-V_{BC}C_{BC}}-\frac{U_{BC}}{U_{CD}C_{CD}}\right]}{\left[\frac{1}{U_{AB}C_{AB}}+\frac{1}{U_{CD}C_{CD}}\right]} \quad (1)$$

Along with electrical measurements, the discharge radiation spectra and spatial radiation distribution were measured. The gas temperature was measured based on the rotational structure of the second positive band of the nitrogen molecule.

Discharges were filmed to study the mechanism of the prolonged discharge formation. Additionally, 4 photodiodes were installed along the working electrode wire at different distances from the ignition electrode, and the time correlation of photodiode signals was studied.

To examine the feasibility of RF atmospheric discharge utilization for the surface modifications of material, samples of different materials were cleaned with ethyl alcohol and were mounted on the plastic layer positioned on the grounded plate. Then, after ignition of the discharge, samples were treated by the plasma during their multiple scans relative to the string. After treatment, contact angle measurements were conducted to evaluate the wettability of samples. In adhesion tests, the peel strength necessary to disassemble 3M Scotch tape attached to the treated samples surface was measured.

Experimental Results and Discussion

Description and general behavior of discharge

The volt-ampere characteristics of the 13.6MHz pin-plate discharge is shown in Fig. 4a. It is worth noting that in order to measure the voltage-ampere(VA) curve, the power of the RF generator was increased incrementally and corresponding values of RF voltage and current registered. The sections of the VA characteristics corresponding to increasing values of RF power are represented by letters in ascending order, starting from A.

The section AB of the VA curve corresponds to no discharge. After ignition of the discharge at point B, the discharge voltage declines. During section CD, the glowing part of the discharge originating near the pin does not touch the plate. The discharge current is sustained by the flow of negative ions and displacement current. At point D, the discharge touches the plate and a sheath between the plasma and electrode is created. A decrease of the discharge RF voltage takes place at this point. At point F, the pin changes its color to red due to heating. The RF current represented in Fig. 4(a) is the total discharge current. Figure 4(b) illustrates the dependence of the active part of the discharge current on discharge voltage. After filling the space between the pin and plate by the plasma (point D), an increase of RF power results in an active current increase and a discharge RF voltage decrease. Thus a stable discharge mode with a negative differential resistance was observed. Most likely, the heating of the gas, the contraction of the discharge channel, thermal electron emission from the pin and an increase of the sheath area contribute to the appearance of this mode.

The potential difference between the plasma and electrodes calculated according to formula 1 demonstrates that the pin and plate have negative potential (about –100 V and –10 V respectively) in relation to the plasma. This potential fall causes the increasing

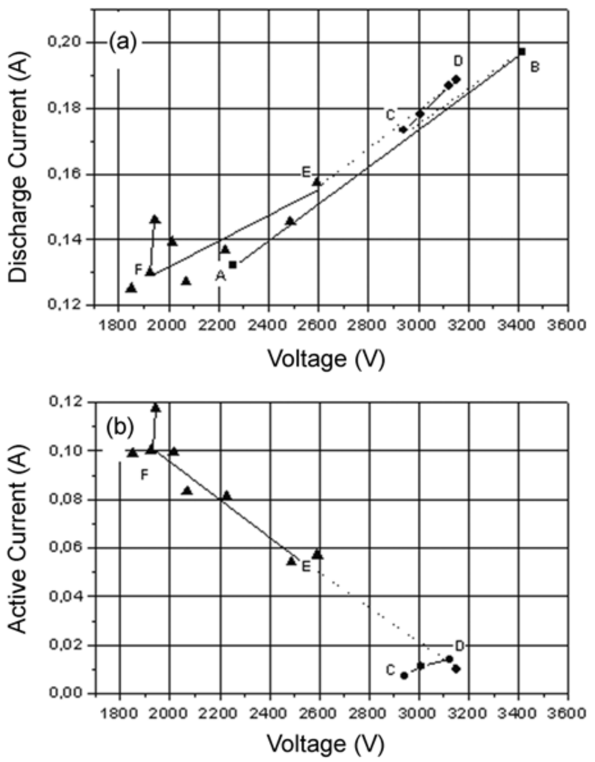

Fig. 4. VA characteristics of the 13.6 MHz pin-plate discharge. (a) total discharge current, (b) active discharge current.

irradiance in near-electrode areas. Spectral measurements showed that when the discharge is concentrated only near the pin, the concentration of nitrogen molecules and molecular ion radiation are maximal near the pin and decrease monotonically with increased distance from the pin. As the discharge occupies the whole gap between pin and plate, a second maximum of radiation appears near the plate (see Fig. 5).

The presence of a dielectric layer between metal plate and discharge does not qualitatively change the observed situation. The appearance of the second radiation maximum can be attributed to the formation of the sheath near the plate. The presence of the sheath near the plate where the samples under treatment are to be located illustrates that one of the important factors of sample treatment under atmospheric pressure is its irradiation by fast ions accelerated in the sheath similar to that in low pressure plasma.

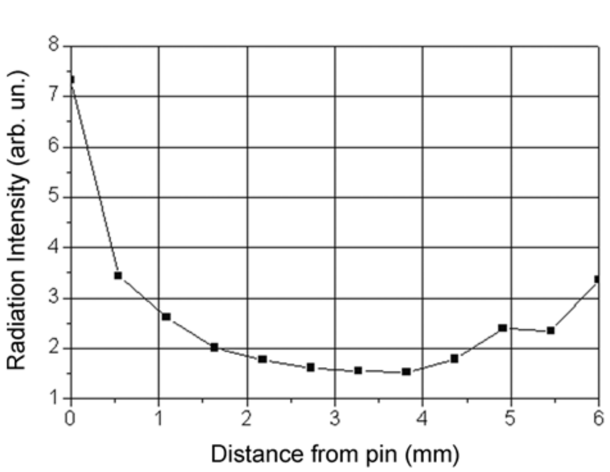

Fig. 5. Dependence of discharge radiation intensity on the distance from the pin.

Frequency effect on discharge behavior

The difference between 13.6 MHz and 0.6 MHz discharges displays itself in that the dependence of the active discharge RF current on time is close to sinusoidal. A weak anharmonicity was observed only at a small distance between pin and plate (see Fig. 6).

The situation is quite different with the 0.6 MHz discharge. Even the appearance of 0.6 MHz and 13.6 MHz pin-pate discharges are quiet different, i.e. the discharge at 0.6 MHz has an evident filamentary structure while the discharge at 13.6 MHz, even under a relatively low air flow (near 10 m/s) is a flame one and no separate filaments can be seen. Typical time dependencies of the 0.6 MHz discharge voltage and active current are shown in Fig. 7, representing significant anharmonicity of the active current. Under conditions

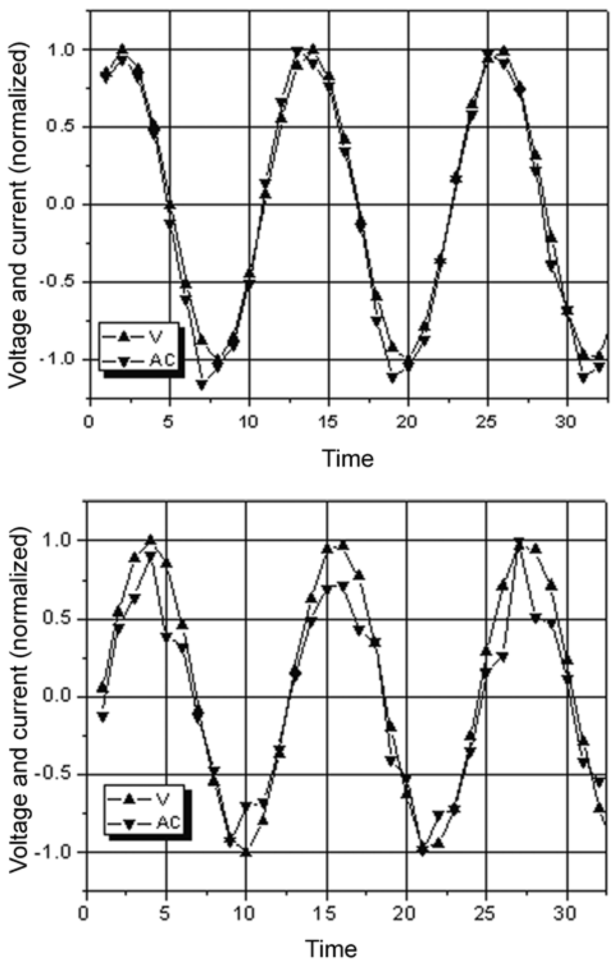

Fig. 6. Ocsilloscope trace of voltage(V) and active current(AC) normalized to the peak. 13.6 MHz discharge, discharge length of 5 mm.

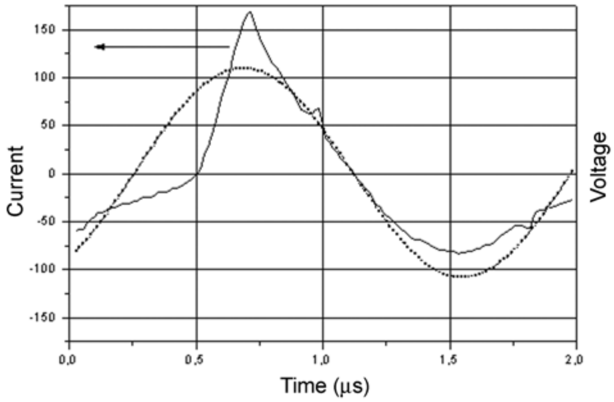

Fig. 7. Trace of the voltage and active current for the 0.6 MHz discharge.

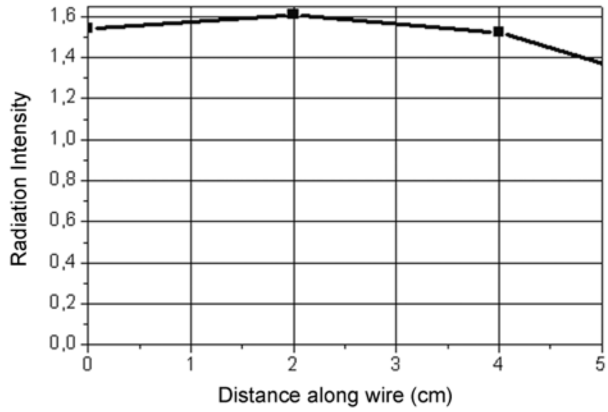

Fig. 9. Longitudinal dependence of radiation intensity.

when the pin has a positive potential relative to the plate, the breakdown of the discharge gap takes place during each period of RF power.

The difference between 13.6 MHz and 0.6 MHz wire-plate discharges is evidenced by the prolonged discharge formation. Results of the video recording of the 13.6 MHz discharge are shown in Fig. 8. An inital flame ignition takes place in the vicinity of the ignition electrode. Then, due to the airflow, the flame moves along the wire. After reaching the end of the wire, the discharge turns off and the next one is ignited by the ignition electrode. An increase of transverse gas velocity leads to an increase of the discharge repetition frequency. These results were confirmed in experiments with photodiodes distributed along the discharge. The time differences between current pulses of the photodiodes were proportional to the distance between them and inversely proportional to the gas velocity.

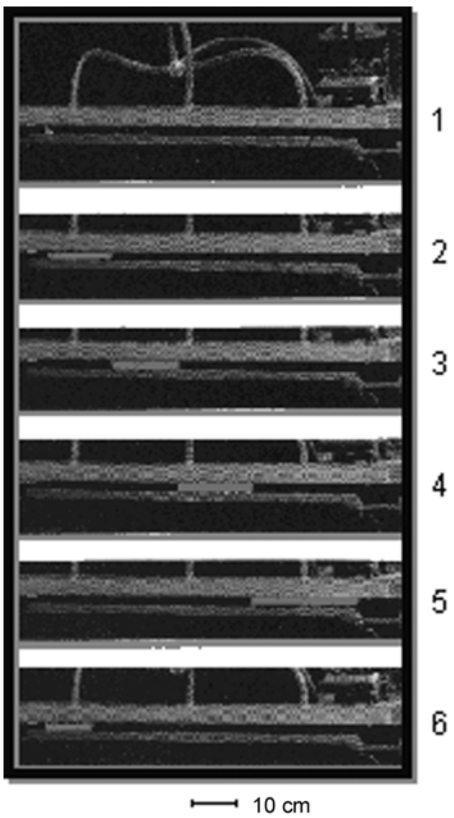

Fig. 8. A video record of discharge at 13.6 MHz. The time difference between pictures is 40 ms.

The situation is different for thet 0.6 MHz discharge with a low airflow rate. Photodiode signals were randomly distributed in time, meaning that discharge areas are distributed randomly along the string and do not change their position due to gas flow. The lifetime of each microdischarge is about 10-20 ms, after its disappearance the next discharge appears at different points along the string. Increased RF power leads to the simultaneous existence of several microdischarges. A significant airflow increase (50-100 m/s) with a 0.6 MHz prolonged discharge results in a formation similar to that typical for 13.6 MHz.

The measurements of intensity averaged in time of discharge radiation showed a high homogeneity of the prolonged RF discharge in all the mentioned modes of its maintenance (see Fig. 9). An increased gas flow leads to the homogenizing of the discharge radiation in the gap between the electrodes. The same trend is typical for gas temperature. Figure 10 shows the distribution of gas temperature as a function of distance normal to the plate. At the minimal operating gas flow, the discharge burning has a bulk character, and the temperature maximum is achieved in the middle of the discharge space, greatly decreasing towards a cold plate. The rapid removal of charged particles, caused by the increasing gas flow, hinders the heating beside the string area, with the gas temperature smoothly decreasing from string to plate.

Frequency effect on polymers surface modification

Improvement of the adhesion of polytetrafluorethylene (PTFE) in air discharge at atmospheric pressure was carried out in RF discharges with working frequencies of 0.6 and 13.6 MHz. The results obtained with the 13.6 MHz discharge treatment of PTFE are present-

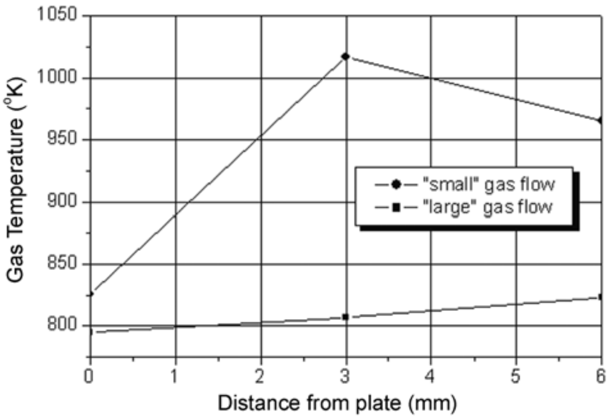

Fig. 10. Dependence of gas temperature on distance from the plate.

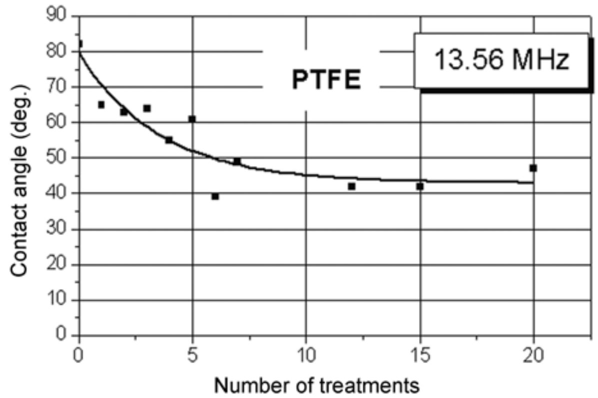

Fig. 11. Dependence of contact angle of PTFE on the scan number. 13.6 MHz discharge.

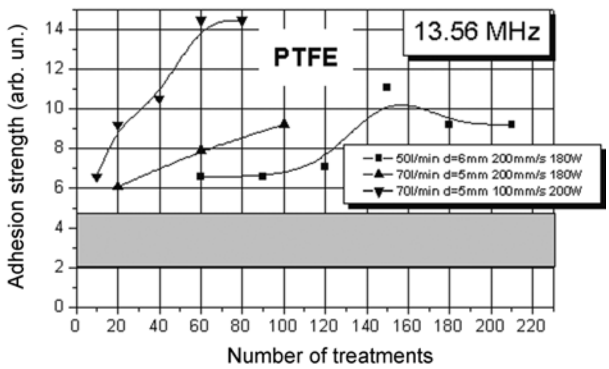

Fig. 12. Dependence of adhesive strength of PTFE samples on treatment number. 13.56 MHz discharge. The gray bar represents the range of adhesive strength values of untreated PTPE samples.

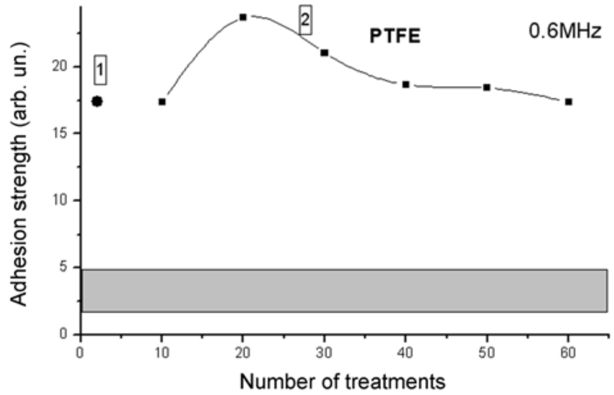

Fig. 13. Dependence of adhesive strength of PTFE samples on treatment number. 0.6 MHz discharge. The gray bar represents the range of adhesive strength values of untreated PTPE samples.

ed in Figs. 11, 12. An adhesive improvement of PTFE is possible but a very large number of scans is necessary. The number of scans can be reduced by increasing the airflow rate, i.e. by increasing the running flame speed and decreasing the speed of sample movement. Surface analysis of the treated samples showed a large deficiency in fluorine, leading to adhesive improvement on the surface, but the surface treatment was not uniform.

In order to improve the situation, the 0.6 MHz discharge with the smallest airflow rate was used. The results obtained are presented in Fig. 13. Using this method, the number of treatments was reduced and the adhesive strength was increased substantially. Unfortunately, due to drawbacks in the line drive system construction, small line drive velocities were impossible.

Experiments demonstrated that sample processing in the discharge decreased the wetting angles of PTFE, polyethylene (PE), polyimide (PI) and polyvinylchloride (PVC) to 40^o, 20^o, 20^o and 25^o, respectively, and the adhesion of PTFE was improved four fold. The treatment of samples was uniform due to the homogeneity of discharge.

Conclusions

A systematic study of atmospheric 0.6 MHz and 13.6 MHz discharge parameters together with results of the influence of the discharge on the wettability and adhesive force of materials surfaces were obtained.

Discharge at 0.6 MHz has evident filamentary structure while discharge at 13.6 MHz has no separate filaments. A significant airflow increase at 0.6 MHz prolonged the discharge results in a mechanism similar to that at 13.6 MHz. The homogeneity of the prolonged RF discharge in all the mentioned modes of its maintenance is high. An increase of gas flow leads to homogenizing of the discharge and gas temperature in the gap between the electrodes.

The dependence of active discharge RF current on time is close to sinusoidal, but the 0.6 MHz discharge represents a significant anharmonicity of active current.

Surface analysis of the 13.6 MHz discharge-treated samples showed a high deficiency in fluorine, leading to adhesive improvement on the surface, but surface treatment was nonuniform. In the 0.6 MHz discharge, the adhesive strength increased substantially.

As a result of samples processing in the discharge the wetting angle of the PTFE, PE, PI and PVC decreased to 40^o, 20^o, 20^o and 25^o, respectively, and the adhesion of PTFE was improved 4 fold. The treatment of samples was uniform due to discharge homogeneity.

Acknowledgement

This work was supported by the Grant No. M1-0104-00-0071 from the National Research Laboratory Program of the Ministry of Science and Technology and Grant R-2004-096-0-00 from the Ministry of Commerce, Industry and Energy, Korea.

References

1. A.P. Napartovich. Plasmas and Polymers 6[1/2] (2001).
2. Jong-kyu Park, Won-tae Ju, Kwang-hyun Paek, Yong-hwan Kim, Yoon-ho Choi, Ji-hun Kim, and Yong-seok Hwang, Surface and Coatings Technology 174-75 (2003) 547-552.
3. E.A. Kralkina, V.A. Riaby, V.P. Savinov, and A.V. Stepanov, Proceedings of IV International Conference “Plasma Physics and Plasma Technologies”, Minsk, September 15-19 (2003) 74-77.